Laser Chem. 1986, Vol. 6, pp. 15-35
0278-6273/86/0601-0015$12.00/0

Printed in Great Britain

INTERNAL ENERGY DISTRIBUTION IN MgO($a^3\Pi$) FORMED FROM Mg(^3P) + O_2 AND N_2O : A CASE OF POPULATION INVERSION

BERNARD BOURGUIGNON, JOELLE ROSTAS, GUY TAIEB, MOHAMMED-ALI GARGOURA and JUNE McCOMBIE

Laboratoire de Photophysique Moléculaire CNRS[≠]
Bâtiment 213 - Université de Paris-Sud
91405 - ORSAY CEDEX France.

ABSTRACT

The internal state distribution of MgO($a^3\Pi$) formed from Mg(^3P) + O_2 and N_2O reactions was determined from a reanalysis of the laser induced fluorescence spectra of the $d^3\Delta$ - $a^3\Pi$ system previously published by Dagdigian. The MgO($a^3\Pi$) state formed in the reaction with O_2 has a quasi-Boltzmann distribution. In the N_2O reaction the rotational excitation is much greater and the vibrational population distribution is inverted with a maximum at v = 2 - 3. The $a^3\Pi$ rovibrational population distributions are compared with those of the $X^1\Sigma^+$ ground state. The dynamics of these reactions are discussed on the basis of earlier ab-initio calculations and experimental data.

≠ Laboratoire associé à l'Université de Paris-Sud.

1. INTRODUCTION

The reactivity of excited magnesium atoms with oxydants has been the subject of numerous recent investigations [1-11]. These studies were carried out in order to understand the primary oxydation process of simple highly exothermic systems expected to produce high energetic (chemiluminescent) electronic states of magnesium oxide, which are easily tractable by emission spectroscopy. However, up to now, it was found that the radiative states are either not or only slightly populated in these reactions and therefore the knowledge of internal energy distribution requires probing dark electronic states.

In 1982, Paul Dagdigian investigated the reactions of metastable $Mg(3s3p\,^3P^0)$ atoms with O_2 and N_2O under single collision conditions by the laser fluorescence technique [5]. He was able to detect the MgO reaction product in the ground $X\,^1\Sigma^+$ and low lying $a\,^3\Pi$ and $A\,^1\Pi$ excited states. The relative populations in the first six vibrational levels of the $X\,^1\Sigma^+$ state and a rotational temperature (T_{rot}) characterizing the rotational distribution in $v_X = 0$ level were determined from (B-X) excitation spectra. The population of the $A\,^1\Pi$ state was found to be very low. The lack of spectroscopic data pertaining to the triplet states precluded any reliable population analysis of the $a\,^3\Pi$ state. We have recently carried out the spectroscopic analysis of bands involving the MgO $a\,^3\Pi$ state, namely the $B\,^1\Sigma^+ - a\,^3\Pi$ and $D\,^1\Delta - a\,^3\Pi$ [12] $d\,^3\Delta - A,a\,^{1,3}\Pi$ [13,14] and $c\,^3\Sigma^+ - a\,^3\Pi$ bands [15]. In this paper, the detailed analysis of the d-a ($\Delta v = 0$) system at 372 nm is used to interpret Dagdigian's [5] spectrum of nascent

$MgO(a^3\Pi)$ formed in the $Mg(^3P) + N_2O$ and O_2 reactions. Although the heavy overlap of the d-a ($\Delta v = 0$) bands precludes a definitive quantitative analysis, a semi quantitative population analysis could be achieved. The main results are :

1) For the $Mg + N_2O$ reaction the vibrational population shows a marked maximum at v = 2-3, the rotational excitation is very high, and the $a^3\Pi_2$ component population is anomalously small compared to the two other spin-orbit components. In contrast, the $X^1\Sigma^+$ state presents a smooth vibrational population distribution and a much colder rotational excitation [5]. These results are discussed on the basis of the *ab initio* potential energy surfaces (PES) which have been calculated for the $Mg + N_2O$ system by Yarkony [16]. We show that these population distributions are consistent with the mechanism suggested by Yarkony.

2) For the $Mg + O_2$ reaction, the $MgO(a^3\Pi)$ state shows very low ro-vibrational excitation.

2. POPULATION ANALYSIS

A recent investigation of the UV laser excitation spectrum of MgO produced in a Broida oven provided new reliable spectroscopic data on the triplet manifold, in particular on the $d^3\Delta$ and $c^3\Sigma^+$ [12-15] states. One of the most intense features in the spectrum is the very congested $d^3\Delta - a^3\Pi$ band system at 372 nm which has thus far eluded complete rotational analysis. From appropriate spectrum simulation and partial rotational analysis, we have been

able to show [13] that the four peaks observed at 372.139, 372.094, 372.064 and 372.056 nm are not the Q_1, Q_2, Q_{3e}, Q_{3f} heads of the d-a(0-0) band as previously reported in the literature, [17,18] but the Q_1 ($d^3\Delta_3$ - $a^3\Pi_2$) heads of the (0-0), (1-1), (2-2) and (3-3) bands respectively. Furthermore, the vibrational parameters of $d^3\Delta_3$ and $a^3\Pi_2$ recently determined from the observation of the $d^3\Delta_3$ - $a^3\Pi_2$ ($\Delta v = -1$) sequence by laser excitation [14] show that Q_1(4-4), (5-5), (6-6), (7-7) heads lie below the Q_1 (3-3), (2-2), (1-1) and (0-0) heads respectively. The Q_1 $\Delta v = 0$, for v = 2-5 form a head Q_1^H at 372.1 nm. Such a heavy overlap of eight sequence bands, added to the complex structure of a $^3\Delta$ - $^3\Pi$ transition makes the d-a system inappropriate for vibrational and rotational population analysis. There is, however, a fortunate circumstance in that the effective B_v values for the $a^3\Pi_2$ and $d^3\Delta_3$ components are so close that most of the lines of each $\Delta v = 0$ Q_1 branch fall within one wavenumber, and form an intense and narrow peak. In contrast to the Q_2 and Q_3 heads, the Q_1 heads of the $\Delta v = 0$ sequence are well separated from the other branches of the (d-a) system so that it is possible to estimate the vibrational population distribution of the $a^3\Pi_2$ component from their relative intensities. In addition, the relative intensity of the Q_1 heads with respect to the (Q_2, Q_3) head provides a reliable measure of the $a^3\Pi_2$ relative population with respect to ($a^3\Pi_1$,$a^3\Pi_0$) . Spectral simulation was used to estimate the rotational population assuming a Boltzmann distribution. The validity of this procedure is severely limited for the following reasons :

i) the inaccuracy of the $d^3\Delta$ and $a^3\Pi$ [19] states distortion parameters which have been derived from relatively low temperature spectra ($J < 50$). ii) the lack of data on the $d^3\Delta$ and $a^3\Pi$ $v \geqslant 2$ vibrational levels and iii) the heavy overlap of the bands of the $\Delta v = 0$ sequence.

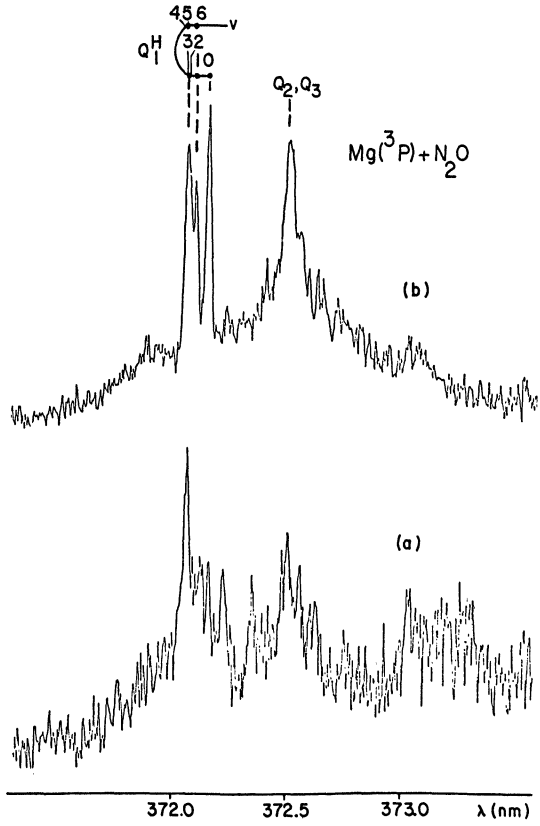

FIGURE 1 - Laser excitation spectrum of Dagdigian [5] for the $d^3\Delta$ - $a^3\Pi$, $\Delta v = 0$ band system of MgO formed in the $Mg(^3P) + N_2O$ reaction. The Q_1 ($d^3\Delta_3$ - $a^3\Pi_2$) heads form a head at 372.1 nm marked Q_1^H. The N_2O scattering gas pressure was (a) 2.5 and (b) 8 mTorr.

The $Mg(^3P) + N_2O$ reaction

Dagdigian recorded the laser excitation spectrum of the 372 nm $d^3\Delta - a^3\Pi$ system for two different N_2O scattering gas pressures [5]. At low pressure (2.5 mTorr of N_2O) the spectrum exhibits three main features (Figure 1a).

1. the most intense peak lies at 372.1 nm and is therefore Q_1^H, formed by the superposition of the $Q_1(v\text{-}v)$ heads with v = 2-5 ; the $Q_1(1\text{-}1)$ head is weak and $Q_1(0\text{-}0)$ is hardly seen. The corresponding population distribution is clearly non Boltzmann. The relative vibrational populations can be estimated from the relative intensities of Q_1^H, $Q_1(1\text{-}1)$ and $Q_1(0\text{-}0)$; these are about 1, 0.15, and 0.04, respectively, for the v = 2-5, v = 1 and v = 0 levels of the $a^3\Pi_2$ component. Assuming that $a^3\Pi_{oe}$, $a^3\Pi_{of}$ and $a^3\Pi_1$ behave as the $a^3\Pi_2$ component and using the total branching ratio between $a^3\Pi$ and $X^1\Sigma^+$ determined by Dagdigian (Table 1), we obtained the $a^3\Pi$ vibrational populations normalized to 1 for the sum of the $X^1\Sigma^+$ vibrational levels given in Table 1. To get further insight, the population distribution was modelled to a Gaussian profile, which then shows a maximum for v = 2-3. The vibrational population distributions of the $X^1\Sigma^+$, $a^3\Pi$, and $A^1\Pi$ states are shown schematically in Figure 2.

2. The intensity of the Q_1 heads relative to the (Q_2, Q_3) head is notably smaller than expected, indicating that the formation of the $a^3\Pi_2$ component is less favoured than the others. Since the Q_2, Q_3 heads

TABLE 1 - Internal energy distribution of MgO formed from $Mg(^3P) + N_2O$ [a]

	$X^1\Sigma^+$ [b]		$a^3\Pi$ [c]		$A^1\Pi$ [b]
Electronic branching ratio	0.33		0.43 [b]		> 0.04
Vibrational branching ratio [d]	v				
	0	0.19 ± 0.02	≤ 0.04 ± 0.04	0.04 [e]	
	1	0.23 ± 0.02	0.17 ± 0.07	0.19	
	2	0.20 ± 0.02		0.43	
	3	0.19 ± 0.02	1.1 ± 0.1	0.43	
	4	0.14 ± 0.02		0.19	
	5	0.05 ± 0.02		0.04	
Electronic energy (cm^{-1})	0		2550		3503
E_{vib} (cm^{-1}) [f]	1600		1400		-
E_{rot} (cm^{-1}) [g]	500		1700		-
Excess energy (ev) [h]	4.2		3.8		

a) *The $(b)^3\Sigma^+$ state calculated at ∿ 8000 cm^{-1} above the ground state may also be formed, but has still not been identified spectroscopically.*

b) *From ref. (5).*

c) *This work.*

d) *Normalised to 1 for the sum of the $X^1\Sigma^+$ vibrational levels.*

e) *Relative populations derived assuming a Gaussian distribution.*

f) *E_{vib} is the mean vibrational energy, defined as $\sum_v v\omega N(v) / \sum_v N(v)$*

g) *$E_{rot} = kT_{rot}$*

h) *The excess energy is the energy available in translation and N_2 vibration-rotation.*

are not separated, the $^3\Pi_1$ and $^3\Pi_0$ components were assumed to be equally populated. Comparison of spectrum 1a with simulated $d^3\Delta$ - $a^3\Pi$ (2-2) bands then yielded the relative populations 0.25 ± 0.10 : 1 : 1 for the $a^3\Pi_2$, $a^3\Pi_1$ and $a^3\Pi_0$ component respectively.

3. High J (up to J ≃130, T_{rot} ≃ 2300 K) rotational levels must be populated in order to account for the considerable rotational structure observed in the

spectrum. This structure shows distinct peaks which are most likely the result of fortuitous overlaps, which are difficult to reproduce for the reasons given above. Therefore, it is not possible to determine whether or not the rotational population follows a Boltzmann distribution.

Table 1 summarizes all available data pertaining to the internal energy distribution of MgO formed from $Mg(^3P) + N_2O$ with an N_2O scattering gas pressure of 2.5 mTorr.

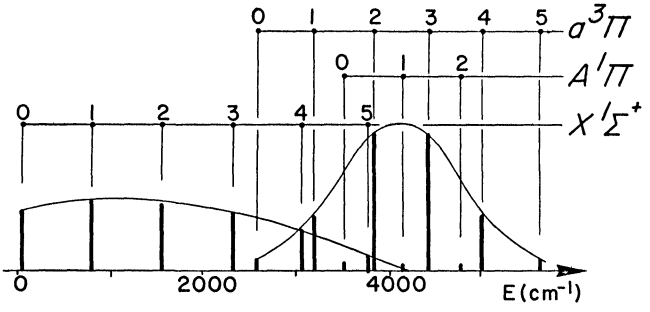

FIGURE 2 - Vibrational population distribution of MgO formed in the $Mg(^3P) + N_2O$ reaction. The total branching ratio between $X^1\Sigma^+$ and $a^3\Pi$ and the vibrational population for $X^1\Sigma^+$ and $A^1\Pi$ are taken from Dagdigian [5]. The $a^3\Pi$ relative population in the v = 0-5 levels have been determined in the present work from the Q_1 head relative intensities (Figure 1a) assuming a Gaussian distribution and are really the $a^3\Pi_2$ relative populations.

The $Mg(^3P) + O_2$ reaction

The MgO ($d^3\Delta - a^3\Pi$) excitation spectrum given by Dagdigian (Figure 3) was recorded at an O_2 pressure of 4 mTorr. At this pressure, it is likely that rotational and vibrational relaxation occurs and therefore the spectrum does not quite reflect the MgO nascent population. In contrast with the spectrum observed for the N_2O reaction, the relative populations follow more or less a Boltzmann distribution ; the Q_1 relati-

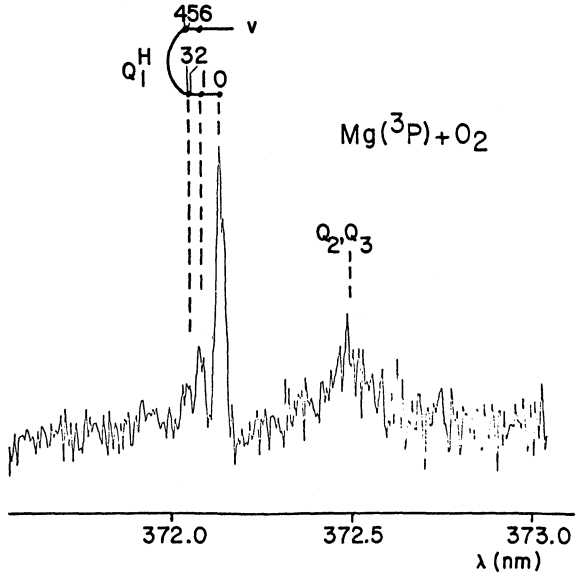

FIGURE 3 - Laser excitation spectrum of Dagdigian [5] for the $d^3\Delta - a^3\Pi$, $\Delta v = 0$ band system of MgO formed in the $Mg(^3P) + O_2$ reaction. The O_2 scattering gas pressure was 4 mTorr.

TABLE 2 - Internal energy distribution of MgO formed from $Mg(^3P) + O_2$ [a]

		$X^1\Sigma^+$ [b]	$a^3\Pi$ [c]
Electronic branching ratio		1.0	0.03 ± 0.01 [b]
Vibrational branching ratio [d]	v		
	0	0.54 ± 0.02	0.020 ± 0.004
	1	0.27 ± 0.02	0.007 ± 0.003
	2	0.13 ± 0.02	< 0.004 ± 0.002
	3	0.04 ± 0.01	
	4	0.02 ± 0.01	
Electronic energy (cm^{-1})		0	2550
E_{vib} (cm^{-1}) [e]		570	310
E_{rot} (cm^{-1}) [f]		1040	-
Excess energy (eV) [g]		1.0	< 0.9

a) The $(b)^3\Sigma^+$ state calculated at ∿ 8000 cm^{-1} above the ground state may also be formed, but has still not been identified spectroscopically. The $A^1\Pi$ state was not observed.

b) From ref. (5).

c) This work.

d) Normalised to 1 for the sum of the $X^1\Sigma^+$ vibrational levels.

e) E_{vib} is the mean vibrational energy, defined as $\sum_v v\omega N(v) / \sum_v N(v)$

f) $E_{rot} = kT_{rot}$

g) The excess energy is the energy available in translation and N_2 vibration rotation.

ve intensities lead to populations in the ratio 1 : 0.35 : 0.10 for v = 0, 1 and 2 respectively. The populations normalized to that of the $X^1\Sigma^+$ state are given in Table 2 along with all of the available data regarding the internal energy of MgO formed from $Mg(^3P) + O_2$. In this case, there is no evidence for a spin-orbit population selectivity. The rotational

excitation is much lower here ($J_{max} \simeq 30-60$) than in the N_2O reaction. Figure 4 shows a schematic representation of the vibrational population distributions for the $X^1\Sigma^+$ and $a^3\Pi$ states of MgO formed in the $Mg(^3P) + O_2$ reaction.

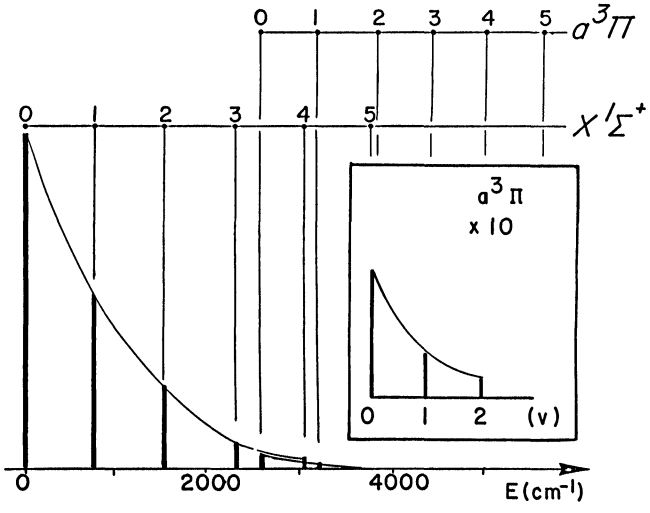

FIGURE 4 - Vibrational population distribution of MgO formed in the $Mg(^3P) + O_2$ reaction. The branching ratio between $X^1\Sigma^+$ and $a^3\Pi$ and the vibrational population for $X^1\Sigma^+$ are taken from Dagdigian [5]. The $a^3\Pi$ relative populations have been determined from the Q_1 head relative intensities (Figure 3).

3. DISCUSSION

The $Mg(^3P) + N_2O$ reaction

The results obtained from nascent MgO laser excitation spectra presented in Table 1 can be summarized as follows. The MgO reaction product is detected in the $X^1\Sigma^+$, $a^3\Pi$ and $A^1\Pi$ states, but not in the as yet unidentified $(b)^3\Sigma^+$ state nor in the higher (chemiluminescent) states, although these are energetically accessible. The relative formation rates are 0.33, 0.43 and $\gtrsim 0.04$ for the $X^1\Sigma^+$, $a^3\Pi$ and $A^1\Pi$ states respectively [5]. The $a^3\Pi$ state is rotationally "hotter" than the $X^1\Sigma^+$ state ($T_{rot} \sim 2300$ K and 700 K respectively). Although the vibrational population distribution is smooth in the $X^1\Sigma^+$ state, it is sharply peaked at v = 2-3 in the $a^3\Pi$ state (Figure 2). Such a contrast in the rovibrational population distributions suggests that the $X^1\Sigma^+$ and $a^3\Pi$ states are formed through different reaction paths.

Yarkony [16] has recently investigated the lowest singlet $1^1A'$ and triplet $1^3A'$ potential energy surfaces (PES) of the Mg + N_2O system using *ab initio* SCF, two configuration MCSCF and CI wavefunctions. The relevant PES's, as calculated by Yarkony, are schematically represented in Figure 5. According to these calculations, the collinear approach of Mg along the N_2O internuclear axis is favoured ; a high potential barrier makes the abstraction mechanism , i.e. direct removal of the O atom from N_2O in a side - on attack, unlikely for both the $Mg(^1S) + N_2O$ and $Mg(^3P) + N_2O$ reactions. No estimation of this barrier height has

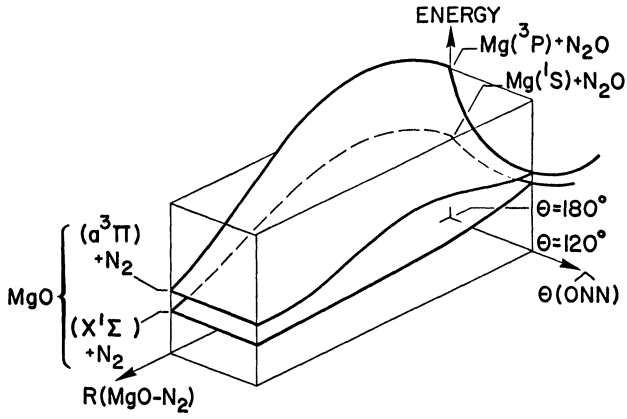

FIGURE 5 - Schematic representation of the lowest PES's of the Mg + N_2O system, summarizing some of Yarkony's results [16]. Potential energy barriers are encountered on the [Energy, R(MgO-N_2)] plane that corresponds to reaction with linear N_2O. N_2O bending allows for a substantial decrease of potential energy. A local barrier is encountered in the exit channel of the triplet surface.

been given. The reaction proceeds via short distance charge transfer from Mg to collinear N_2O, i.e. through a $Mg^+ N_2O^-$ transition state. In the linear configuration N_2O^- is highly excited with respect to the bending vibration. The bending of N_2O^- then allows the reaction to by-pass the potential energy barrier. In the exit channel towards MgO ($a^3\Pi$) + N_2 the system experiences a small ($\sim$ 0.13 eV) local barrier but not in the channel towards MgO ($X^1\Sigma^+$) + N_2 (Figure 6).

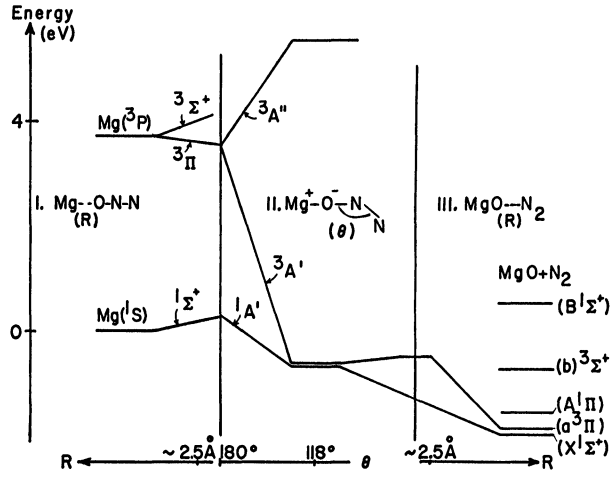

FIGURE 6 - Schematic representation of Yarkony's ab initio calculations on the Mg + N_2O system. The drawing is separated into 3 parts : 1. Collinear approach of Mg and N_2O ($C_{\infty v}$ geometrical constraint). The reaction coordinate is $\sim R(Mg\text{-}ON_2)$. 2. Bending of the $Mg^+ O^- N_2$ transition state (C_s geometrical constraint). The reaction coordinate is $\sim\theta(\widehat{ONN})$. 3. Dissociation of the $Mg^+ O^- N_2$ transition state. The reaction coordinate is $\sim R(MgO\text{-}N_2)$.

Recent theoretical investigations on the dynamics of similar systems (high exothermicity, an intermediate potential well, and no overall potential barrier) predict vibrational population inversion in the products [20]. The expected inversion becomes more pronounced as the intermediate potential well deepens This is supported by experimental results on the exothermic reaction $C(^3P) + N_2O \rightarrow CN + NO$ [21]. An in-

termediate potential well was found in the theoretical calculations and the experimental vibrational population of the CN product was indeed inverted (peak at v = 4). Similarly the MgO ($a^3\Pi$) vibrational distribution obtained in this work is in agreement with the calculated PES characteristics of Yarkony [16] ; i.e. high exothermicity, an intermediate potential well, and no overall barrier. The observation of a hot rotational population of the MgO ($a^3\Pi$) state is consistent with the reaction proceeding through a bent transition state $Mg^+ N_2O^-$ since one expects angular momentum transfer from the transition state bending mode to MgO rotation.

Unlike MgO ($a^3\Pi$), the $X^1\Sigma^+$ ground state does not correlate adiabatically with the $Mg(^3P)$ + N_2O reactants and it must be formed via a non adiabatic transition from the triplet to the singlet surface. This transition may occur either in the transition state region or in the entrance channel. In the first case, the mixing between the two surfaces arising from the same configuration occurs via the spin-orbit interaction, and the formation of the $X^1\Sigma^+$ state is enhanced because of the proximity of the two surfaces in this region (Figure 6). The different vibrational population distribution in the $X^1\Sigma^+$ and $a^3\Pi$ states may be due to the absence of an intermediate potential well on the singlet surface. Additionally such simple considerations cannot explain the very different rotational distributions in the $X^1\Sigma^+$ and $a^3\Pi$ states. As stated above, however, the $1^3A' \rightarrow 1^1A'$ surface transition could occur in the entrance channel, i.e.

in the $C_{\infty v}$ part of the reaction path. This would then be an indirect process going through an intermediate surface, namely the $[Mg^+(^2S) + N_2O^-(^2\Sigma)]^1\Sigma^+$ surface, to the ionic part of the lowest surface (Figure 7). The actual evolution of the system to the $MgO(X^1\Sigma^+) + N_2$ channel in the linear configuration depends on the exact form of the potential surface and the details of the hopping mechanism. These quantities have not been calculated and we can make no definite comment about the smooth vibrational distribution that is actually observed. However to account for the relatively low rotational temperature of the $MgO(X^1\Sigma^+)$ product state the entire reaction would have to be rapid with respect to the bending vibrational time scale of N_2O^-.

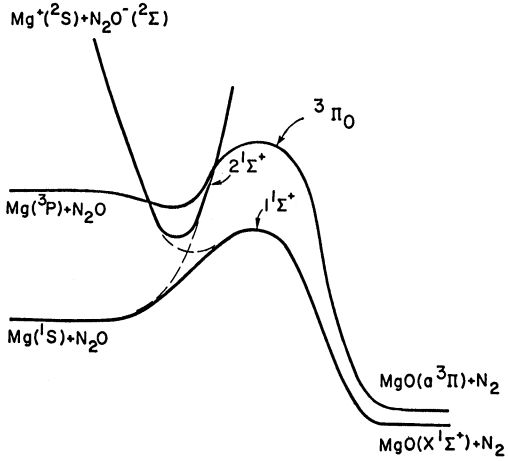

FIGURE 7 - Schematic representation of the reaction path on the lowest $^3\Pi_0$ and $^1\Sigma^+$ surfaces with a $C_{\infty v}$ geometrical constraint. The $1^1\Sigma^+$ ground surface may be reached from the $Mg(^3P) + N_2O$ entrance channel via 2 surface hops $^3\Pi_{0e} \rightarrow 2^1\Sigma^+$ and $2^1\Sigma^+ \rightarrow 1^1\Sigma^+$. height of the barriers is not known.

The Mg + O_2 reaction

The internal distribution of MgO (Table 2) formed from the Mg(^{3}P) + O_2 reaction contrasts sharply in several ways with that of MgO formed from the Mg(^{3}P) + N_2O reaction. MgO is detected in the $X^1\Sigma^+$ and $a^3\Pi$ states but not in the $A^1\Pi$ state. The $X^1\Sigma^+$ state is predominantly populated, the formation rate of $a^3\Pi$ relative to $X^1\Sigma^+$ is only 0.03, i.e. ten times smaller than the calculated statistical rate [22]. The rovibrational excitation is low for both the $a^3\Pi$ and the $X^1\Sigma^+$ states.

In the absence of PES *ab initio* calculations pertaining to this system, Dagdigian [5] inferred that the reaction proceeds through a long-lived $Mg^+O_2^-$ intermediate which lies in a well of $\sim$ 2 eV below the reactants [23,24]. This intermediate which has a C_{2v} structure [25] can dissociate with little orbital rearrangement to the MgO($a^3\Pi$) and MgO($A^1\Pi$) states. In contrast, there is probably a barrier in its decay towards the $X^1\Sigma^+$ ground state of MgO which has a significantly different electronic structure. The rovibrational population distribution observed experimentally depends strongly on the detailed shape of the PES's and can not be quantitatively modelled. The relative low population in the MgO($a^3\Pi$) state may result from non adiabatic transition in the exit channel from the excited triplet to the ground state singlet surface, as suggested previously by Dagdigian [5]. Such non Born-Oppenheimer transition would preferentially depopulate the $a^3\Pi_{oe}$ component [26,27] and therefore the measurement of the relative spin-orbit component

populations would yield evidence for this process. Unfortunately, the resolution of the presently available spectra is too low to provide such data.

4. SUMMARY AND CONCLUSION

The relative populations of $MgO(a^3\Pi)$ formed from $Mg(^3P) + N_2O$ and O_2 under single-collision conditions have been determined from the analysis of the nascent $MgO(d^3\Delta - a^3\Pi)$ spectra reported previously by Dagdigian [5]. The present analysis, based on new spectroscopic data on the triplet states of MgO [12-15], shows that the $MgO(a^3\Pi)$ state formed from the $Mg(^3P) + N_2O$ reaction is characterized by i) a vibrational population inversion : the v = 2-3 levels being the most highly populated, ii) population of high J rotational levels and iii) selective population of the $a^3\Pi$ fine structure levels : the formation of the $a^3\Pi_2$ component is unfavoured. These results contrast with those derived by Dagdigian for the $MgO(X^1\Sigma^+)$ state formed from the same reaction, which shows a smooth vibrational population (v = 0-5) and low rotational temperature (T $\sim$ 700 K). We tentatively explain these profound differences in terms of different reaction paths, as suggested by Yarkony's *ab initio* calculations of selected points on the lowest singlet and triplet A' surfaces. The $a^3\Pi$ rovibrational populations can be rationalized in terms of Yarkony's theoretical results. The high rotational excitation observed for the MgO $(a^3\Pi)$ state arises from its formation through a bent $Mg^+N_2O^-$ transition state. The formation of the $X^1\Sigma^+$ state could possibly

proceed from a similar mechanism followed by a transition from the $^3A'$ surface to the $^1A'$ surface. Alternatively, this state could be formed via an abstraction mechanism (in $C_{\infty v}$ geometry) which would then involve a two step transition to the $^1\Sigma^+$ ground state surface in the entrance channel. For the $Mg(^3P) + O_2$ reaction, the low rovibrational excitation is not inconsistent with the mechanism involving a long-lived MgO_2 intermediate postulated by Dagdigian [5]. More quantitative data on the $MgO(a^3\Pi)$ population distribution could be obtained from appropriate selected fluorescence excitation spectra of the $D^1\Delta - a^3\Pi_1$ and $d^3\Delta_3 - a^3\Pi_2$ transitions which have been observed in bulk conditions and show relatively open rovibrational structure [14]. These spectra are also appropriate for measuring individual rotational line widths which would yield the translational energy. This would be helpful in estimating the N_2 product internal energy. More experimental data will be provided by the experiments under single collision conditions which are in progress in our laboratory [28].

ACKNOWLEDGMENT

It is a pleasure to thank Stephen ROSS for critically reading the manuscript.

REFERENCES

1. G. TAIEB and H.P. BROIDA, J. Chem. Phys. 65, 2914 (1976).
2. F. ENGELKE, R.K. DANDER and R.N. ZARE, J. Chem. Phys., 65, 1146 (1976)
3. D.J. BENARD, W.D. SLAFER and J. HECHT, J. Chem. Phys., 65, 1013 (1977) ; D.J. BENARD and W.D. SLAFER, J. Chem. Phys., 66, 1017 (1977).
4. G. TAIEB, J. Phys. (Paris), 42, 537 (1981).
5. P.J. DAGDIGIAN, J. Chem. Phys., 76, 5375 (1982).
6. J.W. COX and P.J. DAGDIGIAN, J. Phys. Chem., 86, 3738 (1982).
7. B. BOURGUIGNON, J. ROSTAS and G. TAIEB, J. Chem. Phys., 77, 2979 (1982).
8. W.H. BRECKENRIDGE and H. UMEMOTO, J. Phys. Chem., 87, 1804 (1983).
9. H.H. MICHELS and R.A. MEINZER, Chem. Phys. Lett., 98, 6 (1983).
10. R.A. MEINZER, H.H. MICHELS and R. TRIPODI, V Gas Combustion Conference, Oxford (1984).
11. J.W. COX and P.J. DAGDIGIAN, J. Phys. Chem., 88, 2455 (1984).
12. P.C.F. IP, K.J. CROSS, R.W. FIELD, J. ROSTAS, B. BOURGUIGNON and J. McCOMBIE, to be published.
13. B. BOURGUIGNON, J. McCOMBIE and J. ROSTAS, Chem. Phys. Lett., 113, 323 (1985).
14. B. BOURGUIGNON and J. ROSTAS, to be published.
15. B. BOURGUIGNON and J. ROSTAS, VIIth International Symposium on Free Radicals Proceedings (1985).
16. D.R. YARKONY, J. Chem. Phys., 78, 6763 (1983).
17. J. SCHAMPS, Thèse d'Etat Université de Lille (1973).
18. T. IKEDA, N.B. WONG, D.O. HARRIS and R.W. FIELD, J. Molec. Spectrosc., 68, 452 (1977).
19. P.C.F. IP, PhD Thesis, Massachussetts Institute of Technology (1983).

20. M.T. RAYEZ, P. HALWICK, J.C. RAYEZ and B. DUGUAY, to be published.

21. G. DORTHE, M. COSTES, C. NAULIN, J. JOUSSOT-DUBIEN, C. VAUCAMPS and G. NOUCHI, J. Chem. Phys., 83, 3171 (1985).

22. M.H. ALEXANDER and P.J. DAGDIGIAN, Chem. Phys., 33, 13 (1978).

23. M.H. ALEXANDER, J. Chem. Phys., 69, 3502 (1978).

24. M.H. ALEXANDER, unpublished.

25. L. ANDREWS, E.S. PROCHASKA and B.S. AULT, J. Chem. Phys., 69, 556 (1978).

26. B. POUILLY, J.M. ROBBE and M.H. ALEXANDER, J. Phys. Chem., 88, 140 (1984).

27. M.H. ALEXANDER and B. POUILLY, J. Chem. Phys., 79, 1545 (1983).

28. B. BOURGUIGNON, M.-A. GARGOURA and G. TAIEB, to be published.